Molecular Anatomy of Plant Photoprotective Switches: The Sensitivity of PsbS to the Environment, Residue by Residue

Nicoletta Liguori,*,[†] Sara R. R. Campos,[‡] António M. Baptista,[‡] and Roberta Croce*,[†]

[†]Department of Physics and Astronomy, Faculty of Sciences, Vrije Universiteit Amsterdam, De Boelelaan 1081, 1081 HV Amsterdam, The Netherlands

[‡]Instituto de Tecnologia Química e Biológica António Xavier, Universidade Nova de Lisboa, 2780-157 Oeiras, Portugal

Ⓢ *Supporting Information*

ABSTRACT: Under strong sunlight, plants avoid photooxidation by quenching the excess absorbed energy. Quenching is triggered by PsbS, a membrane protein that is activated and deactivated by the light-dependent pH changes in the thylakoid lumen. The mechanism of action of this protein is unknown, but it was suggested that several glutamates act as pH sensors. However, the pK_a of glutamate is several pH units below the physiological values in the lumen. Thus, how can PsbS sense the pH of the lumen, and how does it respond to it? By applying a nonstandard molecular dynamics method that treats pH explicitly, we show that the lumen-exposed glutamates of PsbS have strongly shifted pK_a values and that such shifts are crucial for the pH sensitivity in physiological conditions. We also demonstrate that protonation drives a systematic unfolding of a region key for protein−protein interactions, indicating that PsbS response to pH is a functional conformational switch.
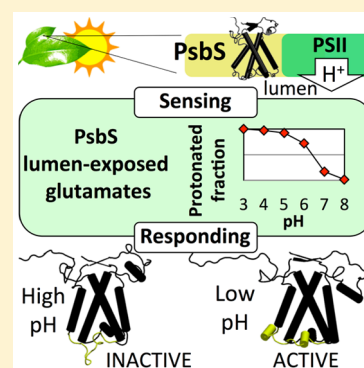
Plants avoid photooxidation by dissipating as heat the energy absorbed in excess in what is called energy-dependent quenching or qE.[1] The light-harvesting complexes (LHCs) are the site of qE.[2] Under low or normal light conditions, the LHCs transfer excitation energy to the core of photosystem II (PSII). Here, photochemistry is initiated and protons are pumped into the thylakoid lumen, an aqueous compartment enclosed by the photosynthetic membrane. Under high light, because of the increased rate of electron transfer, a proton gradient is established between the stromal and lumenal sides of the membrane, with the lumenal pH dropping from ∼7.5 to ∼5.7 (±0.5).[3] A membrane protein named PsbS is activated by the acidification of the lumen[4,5] and triggers qE.[4,6]

The essential role of PsbS in triggering qE in plants was discovered almost 20 years ago,[7] and although several amino acid residues critical for its activity have been identified, its mechanism of action remains elusive. Also, although the crystal structure obtained at pH 5 shows a dimeric complex,[8] it has been suggested that the active form of PsbS (low pH) is monomeric while the dimer is the dominating form at high pH values and is inactive.[4−6,9,10] Furthermore, the overall effect of pH changes on the structure of PsbS is unknown and, to date, only the structure at pH 5 has been resolved.[8]

To understand the structural basis of the pH sensitivity and the effect of pH changes on PsbS, we applied a state-of-the-art method known as constant-pH molecular dynamics (CpHMD).[11,12] CpHMD simulations are able to capture with atomistic resolution the time-dependent structural transitions of proteins at a given pH. In brief, during each CpHMD trajectory, protonation states for the titratable residues of the protein are reset iteratively at given time intervals, depending on the local environment to which each residue is exposed and on the set pH. To do so, CpHMD combines molecular dynamics (MD) simulations with continuum electrostatics (Poisson−Boltzmann or PB) and Monte Carlo (MC) methods. Via the MD simulations, the protein is allowed to rearrange its structure in function of the protonation pattern at a given pH. Via the PB/MC calculations, the protonation pattern is then regularly updated throughout the MD simulation, allowing for the equilibration of the protein structure at the investigated pH value and the collection of quantitative information about the pH sensitivity of every residue. Although the calculation of pK_a values is a challenging task,[13] the CpHMD method has proven to be able to capture (i) the atypical pK_a values that some residues exhibit depending on the local environment,[14] (ii) the coupling between selected protein conformations and protonation states,[12,15] and (iii) the entropy contribution of every possible protonation state at each titratable site.[16]

In this work, the dynamics of a monomer of PsbS in a simulated native-mimicking membrane has been investigated at 6 different pH values ranging from 3 to 8. At each pH value investigated, 5 independent replicas were run for a total of 30 independent simulations and about 5 μs of total simulated time. This titration allowed us to determine the pK_a values of each protonable residue of PsbS and to identify the pH-dependent conformational changes of the protein.
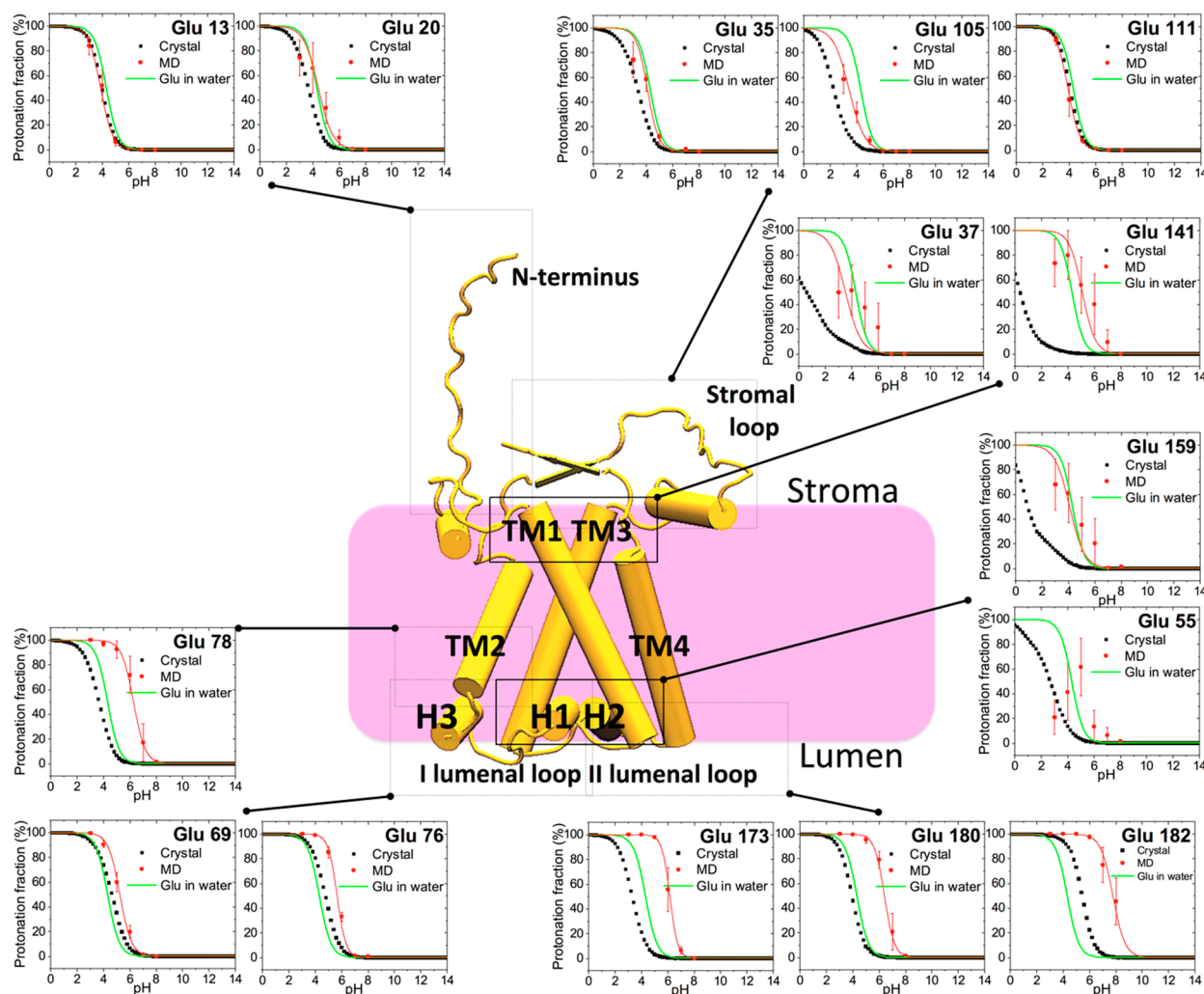
Figure 1. pH sensitivity of PsbS residue by residue: the case of Glu. Titration curves of selected Glu of PsbS exposed to different regions of the protein−membrane environment. The protein structure is reported in gold, and the light magenta box represents the membrane. Each red point in the graphs and the associated error bars were calculated, respectively, as an average and standard error over the 5 independent replicas equilibrated at each pH value (the first 100 ns of each replica was discarded from the analyses). The red solid curve in each graph represents the fit of the CpHMD data using the Hill approximation (see Methods in the Supporting Information).

In order to determine the sensitivity of PsbS to pH, residue by residue, we calculated the frequency of protonation at a given pH for every titratable site over each CpHMD trajectory at equilibrium. By doing so, complete titration curves were reconstructed for the whole set of (protonable) residues. For comparison, the frequency of protonation at the different pH values was also computed on the crystal structure of PsbS[8] embedded in the same equilibrated membrane−water system used for the CpHMD simulations (see Methods in the Supporting Information).

The titration curves for the whole set of titratable amino acids of PsbS are reported in Figure S1. Figures 1 and 2 focus on the glutamic acids (Glu) because several Glu residues have been proposed to be responsible for the pH sensitivity of the protein.[17,18] We found that all of the pK_a values of the stroma-exposed Glu (Glu13, Glu20, Glu35, Glu37, Glu105, Glu111, and Glu141) have a small shift (within one pH unit, Figure 2) from the pK_a of Glu in water (4.3,[19] green curve in Figures 1 and S1). This means that their pK_a values are not strongly influenced by the protein environment and/or the lipid membrane. At striking variance with the stromal side, most of the lumenal exposed Glu have a pK_a that is strongly shifted

with respect to the value in water. These pK_a shifts, up to 3.4 pH units in the case of Glu182 (Figure 2), make the majority of the lumenal exposed Glu (Glu69, Glu76, Glu78, Glu173, Glu180, and Glu182) sensitive to the range of physiological pH values that are critical for the activation of qE. This means that when light saturates the photosynthetic machinery, the lumen-exposed Glu sense the associated change in pH allowing PsbS to respond to light fluctuations. The fact that multiple glutamates contribute to the sensitivity of PsbS is in agreement with experimental results[17] showing that single or double mutations of Glu69, Glu78, Glu173, and Glu182 all resulted in plant lines with reduced qE levels. Our results show that all these residues have pK_a values in the range of the thylakoid lumen. This is not the case for the other two lumen-exposed residues Glu55 and Glu159, which have a very low probability to be protonated at pH > 5. Interestingly, these residues were found to be essential for the proper folding and stability of PsbS.[17] We found that the unprotonated form of these residues, which is present at all physiological pH values, preserves their role in the anchoring of the central transmembrane helices TM1 and TM3 via hydrogen bonds to the
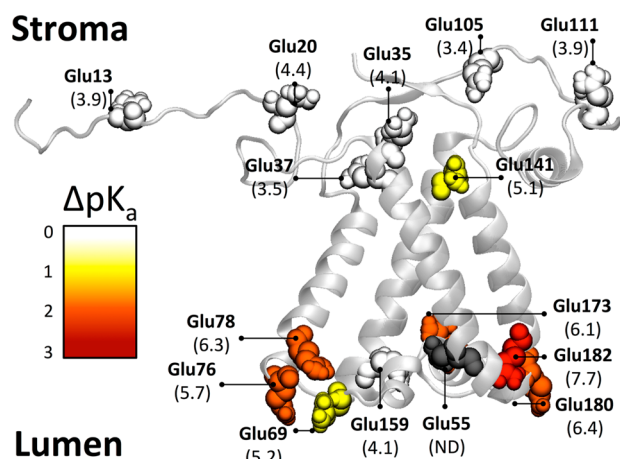
Figure 2. pK_a shifts of PsbS Glu residues. The values reported in parentheses are the pK_a of Glu computed via the CpHMD method by fitting the titration curves of the simulated structures in the Hill approximation (see Methods in the Supporting Information). The different colors associated with the Glu residues represent the difference between the computed pK_a and the standard pK_a value of Glu in water (4.3[19]). pK_a shifts below 0 and above 3 are colored in white and dark red, respectively. Glu residues are shown as van der Waals spheres. Glu55 (shown in gray) does not have a well-defined single midpoint pK_a value (indicated as ND in the figure), as seen in its titration curve (Figure 1).

backbone of H2 and H1,[8] respectively, thus stabilizing the protein (Figure S2A,B).

Large pK_a shifts in proteins are well-studied, including in Glu residues,[20,21] being a common benchmark for pK_a prediction methods.[13] They are caused by desolvation and/or electrostatics, both possibly modulated through pH-dependent structural changes. Desolvation effects occur when a protein ionizable residue is not as exposed to the solvent as it would be when alone in aqueous solution, meaning that its charged form would be less stabilized by surrounding water dipoles and, therefore, the neutral−charged equilibrium would be shifted toward the neutral form. In the case of acidic groups (Glu, Asp, etc.), this would correspond to a pK_a higher than when alone in solution. Therefore, if a Glu residue has a high pK_a due only to desolvation, we would expect its solvent-accessible surface area (SASA) to be unusually low when the residue is neutral (the residue will always tend to get exposed when charged, even though that may happen only at unusually high pH). Figure S3 shows that a reasonable relation is found between SASA and pK_a, except for Glu-37, Glu-141, and Glu-159. Therefore, desolvation seems to explain a part of the observed high pK_a of Glu residues, but electrostatics must also be playing a role.

Electrostatic effects occur when a group experiences substantial electrostatic interactions from other charged groups, either because they are close to it or, if more distant, they can strongly interact through a region of low dielectric constant (e.g., the hydrophobic core of a protein or membrane). In the case of two acidic groups, such an interaction induces a positive pK_a shift and, if they happen to titrate around the same pH region, the shift can be reciprocal, i.e., both groups will increase its pK_a. When these mutual shifts take place, the protonation of the two groups tends to be opposite, i.e, negatively correlated: their joint state is either charged/neutral or neutral/charged. Furthermore, when such strong interactions involve more than two residues, unexpected

positive correlations may occur, with some pairs of groups exhibiting a charged/charged or neutral/neutral joint state, possibly associated with nonmonotonic "up-and-down" titration curves like those of Glu-55 and Glu-141, as experimentally observed in small compounds.[22] The "outliers" in Figure S3, Glu-37, Glu-141, and Glu-159, are indeed found to engage in an extensive network of correlations with multiple residues, as illustrated in Figure S4. Therefore, the high pK_a values of these Glu residues seem to be due to this network of electrostatic interactions.

It is important to note that, without the combination of continuum electrostatics and molecular dynamics (CpHMD), it would not have been possible to predict most of the pK_a shifts, as it can be inferred from the titration curves computed on the crystal (Figures 1 and S1). This difference with the crystal structure strongly suggests that conformational dynamics are crucial in determining the pK_a values of PsbS and, therefore, its functionality.

Similar to the stromal Glu, the aspartate residues, which are all present at the stromal side of PsbS, also showed pK_a shifts of <1 unit with respect to the value in water (Figure S1), meaning that their pK_a values remain outside of the physiologically relevant pH range. The pK_a computed for the other titratable residues considered in this work (lysine and tyrosine) did not show deviation from the values estimated in water and were all above 8 (Figure S1).

We conclude that the ability of PsbS to sense the pH range relevant for the activation of qE, which is 1−3 pH units higher than the standard pK_a of an acid residue, comes from the significant shift in pK_a of its lumenal exposed Glu. This is particularly interesting considering that it has been proposed that the main role of PsbS is to raise the pH at which qE is triggered to a value which is physiologically attainable in the lumen.[23]

What is the response of PsbS to the different pH values? To answer this question, we characterized the conformational space of PsbS at the different pH values. In order to capture the pH-dependent flexibility of PsbS, we computed the pH-dependent root-mean-square fluctuation (RMSF) that is a measure of the conformational freedom of single residues at equilibrium. The sets of RMSFs per different pH values are shown in Figure S5. The RMSF analysis revealed that PsbS is characterized, at all pH values, by a rigid transmembrane region and by highly flexible solvent-exposed domains, namely, the termini and the first (I) and second (II) luminal loops (see Figure 3A for a structural reference). To better distinguish which regions respond to pH, we calculated the root-mean-square deviation (RMSD) per residue of the average protein structures at a given pH with respect to the average structure equilibrated at pH 5, corresponding to the pH value at which the protein was crystallized.[8] The different RMSD profiles are reported in Figure S5. The most substantial deviations were found at the termini and at the I- and II-lumen loops, where the highest RMSF was also found. This means that the apparent deviations from the structure at pH 5 registered at these domains might originate from (i) an intrinsic disorder of these regions which results in high variance at all pH values or (ii) a real deviation from the structure at pH 5.

To discriminate between these possibilities, we determined the equilibrated secondary structure of PsbS at the different pH values. In Figure S6, the frequency of the occurrence of specific types of local structures is reported for each protein domain. The possible types of local structure follow the DSSP
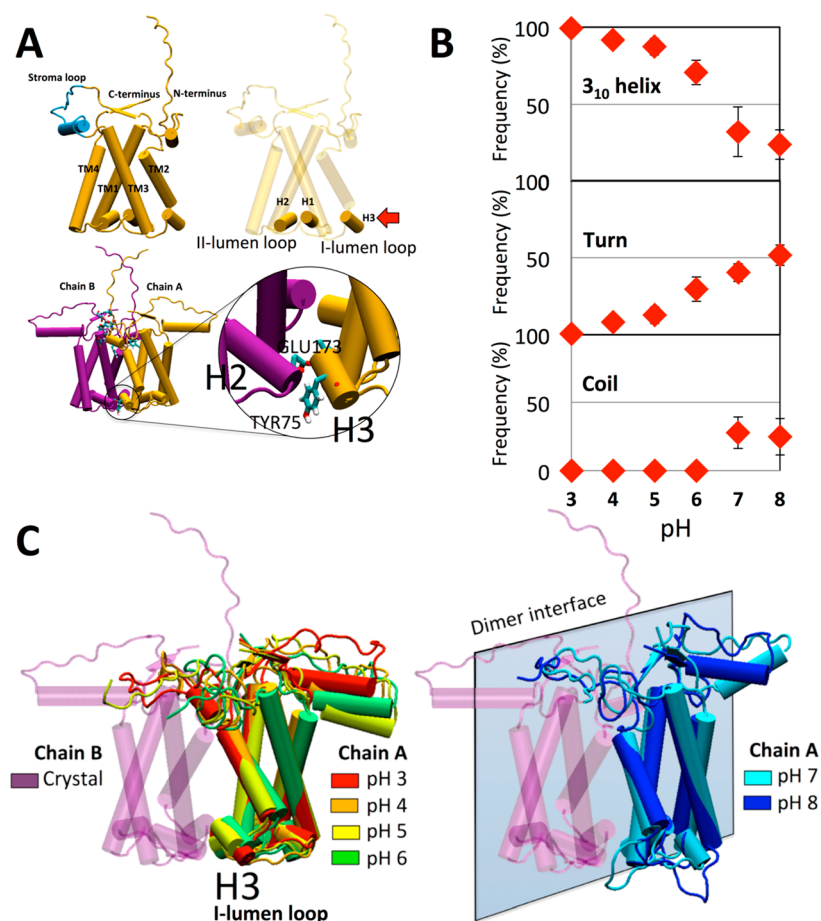
Figure 3. pH-dependent conformational change of PsbS. (A) Crystal structure of PsbS monomeric subunit (chain A, upper) and of PsbS dimer (lower). The amphipathic helices are indicated as well as the network of interactions between H2 and H3 in the inset. In cyan, the sequence reconstructed via the sequence homology model (see Methods in the Supporting Information) is reported. Chain B has been also reconstructed in the figure for the parts not resolved in the original structure.[8] (B) pH-dependent structure of H3. (C) Selected structures of PsbS monomer extracted from the CpHMD at different pH values as indicated in the legend and aligned on top of chain A to the crystal structure of PsbS dimer.

algorithm assignment (see Methods in the Supporting Information) and are 3_{10} helix, α-helix, π-helix, β-bridge, β-sheet, turn, or coil. As reported in Figure S6, we found that, except for the I-lumen loop which contains the short amphipathic helixes H1 and H3 (Figure 3A), all other protein domains largely conserved at every investigated pH value (3–8) the type of secondary structure that they have in the crystal.[8] Among these well-conserved domains are the C- and N-terminus and the II-lumen loop containing helix H2, suggesting that their high RMSD (Figure S5) is due to an intrinsic disorder of these regions without a change of secondary structure. In the case of H1, instead, the simulations showed that the α-helix present in the crystal structure had the tendency to change to either a 3_{10} helix or a turn, but without a clear pH dependence (values of α-helix probability of 99%, 95%, 73%, 62%, 93%, and 84% in the pH range 3–8, respectively).

What then is the response of PsbS to pH? We systematically found that at high pH values (pH 7–8) the helical H3 domain switched to a lumen exposed loop (Figure 3C). In the crystal, H3 is hydrogen bonded via the backbones of Ile74 and Tyr75 to the short amphipathic helix H2 belonging to the other monomer in the PsbS crystal unit[8] (Figure 3A). Fan et al. suggested that these hydrogen bonds are crucial in stabilizing the monomer–monomer interactions.[8] The residue on H2

responsible for the hydrogen bond is Glu173[8] (Figure 3A), one of the putative pH-sensitive sites of PsbS.[17] Interestingly, as shown in Figure S6, protonation of Glu173 did not induce a conformational change in H2, and it conserved (together with the whole second (II) lumen loop) its structure at all pH values. On the other hand, high pH values (7 and 8) induced a complete unfolding of the amphipathic helix H3: this domain changed from a 3_{10} helix to a turn/coil (Figures 3B and S6). The representative conformations of PsbS at the different pH values are reported in Figure 3C.

What could be the functional effect on qE of the conformational switch of PsbS? The change in the structure of the H3 would result in the disruption of the ordered hydrogen bond network that anchors H2 to H3 in the dimer and weaken the interactions between monomers (Figure 3A,C and Supplementary Video 1). Our findings can explain the experimental results of Fan et al., who observed that the lumenal loops of the two PsbS monomers in the dimer are located at a larger distance at high pH.[8]

Because at low pH PsbS is supposed to interact with other LHCs,[6,9,24] we speculated that the creation of a pH-sensitive docking mechanism through a network of tunable electrostatic interactions could be the basis of the mechanism of action of PsbS. Indeed, the alignment of any high-resolution structure of the homologous LHCs[25,26] onto the central helices (the most

conserved elements in the LHC family[27]) of one of the PsbS monomers in the dimeric crystal unit, results in dimers (Figure S7A–C) in which the PsbS H3 domain is facing the lumenal amphipathic helix of the other subunit, i.e., helix 4 for Lhcb and H2 for PsbS in the crystal. Such an organization (amphipathic helix 4 facing the amphipathic helix between the first and second transmembrane helices) is typical of dimeric LHCs in plants (Figure S7D). This would suggest that PsbS can stably dock to LHCs only at low pH, when the H3 is structured (see Supplementary Video 2 for an example of the PsbS dimer at low pH). In this respect, the presence of PsbS dimers in the crystal structure (resolved at pH 5) can be the result of the high capacity of PsbS to interact with other proteins at low pH.

Overall, our work suggests that a conformational reorganization is the basis of the mechanism of action of PsbS in plants. This conformational reorganization is triggered by the protonation of multiple Glu residues exposed to the thylakoid lumen. We found that this is possible because the PsbS design adapted to match the range of physiological pH values of the thylakoid lumen by fine-tuning the pK_a of its lumen-exposed residues.

■ COMPUTATIONAL METHODS

The methods are reported in the Supporting Information.

■ ASSOCIATED CONTENT

Ⓢ Supporting Information

The Supporting Information is available free of charge on the ACS Publications website at DOI: 10.1021/acs.jp-clett.9b00437.

> PsbS monomer aligned to the chain A in the PsbS crystallized dimer and simulated here via CpHMD at pH 8, showing the progressive loss of structure of its I-lumen loop at the interface between the two monomeric subunits, while the II-lumen loop maintains its structure (AVI)

> PsbS monomer aligned to the chain A in the PsbS crystallized dimer and simulated here via CpHMD at pH 5, showing the conservation of structure of its I- and II-lumen loops at the interface between the two monomeric subunits (AVI)

> Fully detailed methods and supplementary figures (PDF)

■ AUTHOR INFORMATION

Corresponding Authors
*E-mail: n.liguori@vu.nl.
*E-mail: r.croce@vu.nl.

ORCID Ⓞ
Nicoletta Liguori: 0000-0001-5695-4012
Sara R. R. Campos: 0000-0003-1020-6830
António M. Baptista: 0000-0002-7044-1210

Notes
The authors declare no competing financial interest.

■ ACKNOWLEDGMENTS

■ REFERENCES

(1) Müller, P.; Li, X.-P.; Niyogi, K. K. Non-Photochemical Quenching. A Response to Excess Light Energy. *Plant Physiol.* **2001**, *125*, 1558–1566.

(2) Ruban, A. V.; Johnson, M. P.; Duffy, C. D. P. The Photoprotective Molecular Switch in the Photosystem II Antenna. *Biochim. Biophys. Acta, Bioenerg.* **2012**, *1817*, 167–181.

(3) Takizawa, K.; Cruz, J. A.; Kanazawa, A.; Kramer, D. M. The Thylakoid Proton Motive Force in Vivo. Quantitative, Non-Invasive Probes, Energetics, and Regulatory Consequences of Light-Induced Pmf. *Biochim. Biophys. Acta, Bioenerg.* **2007**, *1767*, 1233–1244.

(4) Li, X.-P.; Müller-Moulé, P.; Gilmore, A. M.; Niyogi, K. K. PsbS-Dependent Enhancement of Feedback de-Excitation Protects Photosystem II from Photoinhibition. *Proc. Natl. Acad. Sci. U. S. A.* **2002**, *99*, 15222–15227.

(5) Bergantino, E.; Segalla, A.; Brunetta, A.; Teardo, E.; Rigoni, F.; Giacometti, G. M.; Szabò, I. Light- and pH-Dependent Structural Changes in the PsbS Subunit of Photosystem II. *Proc. Natl. Acad. Sci. U. S. A.* **2003**, *100*, 15265–15270.

(6) Wilk, L.; Grunwald, M.; Liao, P.-N.; Walla, P. J.; Kühlbrandt, W. Direct Interaction of the Major Light-Harvesting Complex II and PsbS in Nonphotochemical Quenching. *Proc. Natl. Acad. Sci. U. S. A.* **2013**, *110*, 5452–5456.

(7) Li, X. P.; Björkman, O.; Shih, C.; Grossman, a R.; Rosenquist, M.; Jansson, S.; Niyogi, K. K. A Pigment-Binding Protein Essential for Regulation of Photosynthetic Light Harvesting. *Nature* **2000**, *403*, 391–395.

(8) Fan, M.; Li, M.; Liu, Z.; Cao, P.; Pan, X.; Zhang, H.; Zhao, X.; Zhang, J.; Chang, W. Crystal Structures of the PsbS Protein Essential for Photoprotection in Plants. *Nat. Struct. Mol. Biol.* **2015**, *22*, 729–735.

(9) Bonente, G.; Howes, B. D.; Caffarri, S.; Smulevich, G.; Bassi, R. Interactions between the Photosystem II Subunit PsbS and Xanthophylls Studied in Vivo and in Vitro. *J. Biol. Chem.* **2008**, *283*, 8434–8445.

(10) Krishnan, M.; Moolenaar, G. F.; Gupta, K. B. S. S.; Goosen, N.; Pandit, A. Large-Scale in Vitro Production, Refolding and Dimerization of PsbS in Different Microenvironments. *Sci. Rep.* **2017**, *7*, 15200.

(11) Baptista, A. M.; Teixeira, V. H.; Soares, C. M. Constant-pH Molecular Dynamics Using Stochastic Titration. *J. Chem. Phys.* **2002**, *117*, 4184–4200.

(12) Machuqueiro, M.; Baptista, A. M. Constant-pH Molecular Dynamics with Ionic Strength Effects: Protonation-Conformation Coupling in Decalysine. *J. Phys. Chem. B* **2006**, *110*, 2927–2933.

(13) Alexov, E.; Mehler, E. L.; Baker, N.; Baptista, A. M.; Huang, Y.; Milletti, F.; Nielsen, J. E.; Farrell, D.; Carstensen, T.; Olsson, M. H. M. Progress in the Prediction of pKa Values in Proteins. *Proteins: Struct., Funct., Genet.* **2011**, *79*, 3260–3275.

(14) Machuqueiro, M.; Baptista, A. M. Is the Prediction of pKa Values by Constant-pH Molecular Dynamics Being Hindered by Inherited Problems? *Proteins: Struct., Funct., Genet.* **2011**, *79*, 3437–3447.

(15) Campos, S. R. R.; Machuqueiro, M.; Baptista, A. M. Constant-pH Molecular Dynamics Simulations Reveal a β-Rich Form of the Human Prion Protein. *J. Phys. Chem. B* **2010**, *114*, 12692–12700.

(16) Baptista, A. M.; Soares, C. M. Some Theoretical and Computational Aspects of the Inclusion of Proton Isomerism in the Protonation Equilibrium of Proteins. *J. Phys. Chem. B* **2001**, *105*, 293−309.

(17) Li, X.-P.; Phippard, A.; Pasari, J.; Niyogi, K. K. Structure−function Analysis of Photosystem II Subunit S (PsbS) in Vivo. *Funct. Plant Biol.* **2002**, *29*, 1131−1139.

(18) Li, X.-P.; Gilmore, A. M.; Caffarri, S.; Bassi, R.; Golan, T.; Kramer, D.; Niyogi, K. K. Regulation of Photosynthetic Light Harvesting Involves Intrathylakoid Lumen pH Sensing by the PsbS Protein. *J. Biol. Chem.* **2004**, *279*, 22866−22874.

(19) Grimsley, G. R.; Scholtz, J. M.; Pace, C. N. A Summary of the Measured pK Values of the Ionizable Groups in Folded Proteins. *Protein Sci.* **2009**, *18*, 247−251.

(20) Isom, D. G.; Cannon, B. R.; Castañeda, C. A.; Robinson, A.; García-Moreno E., B. High Tolerance for Ionizable Residues in the Hydrophobic Interior of Proteins. *Proc. Natl. Acad. Sci. U. S. A.* **2008**, *105*, 17784−17788.

(21) Isom, D. G.; Castañeda, C. A.; Cannon, B. R.; Velu, P. D.; García-Moreno E., B. Charges in the Hydrophobic Interior of Proteins. *Proc. Natl. Acad. Sci. U. S. A.* **2010**, *107*, 16096−16100.

(22) Submeier, J. L.; Reilley, C. N. Nuclear Magnetic Resonance Studies of Protonation of Polyamine and Aminocarboxylate Compounds in Aqueous Solution. *Anal. Chem.* **1964**, *36*, 1698−1706.

(23) Johnson, M. P.; Ruban, A. V. Restoration of Rapidly-Reversible Photoprotective Energy Dissipation in the Absence of PsbS Protein by Enhanced ΔpH. *J. Biol. Chem.* **2011**, *286*, 19973−19981.

(24) Teardo, E.; Delaureto, P.; Bergantino, E.; Dallavecchia, F.; Rigoni, F.; Szabo, I.; Giacometti, G. Evidences for Interaction of PsbS with Photosynthetic Complexes in Maize Thylakoids. *Biochim. Biophys. Acta, Bioenerg.* **2007**, *1767*, 703−711.

(25) Pan, X.; Li, M.; Wan, T.; Wang, L.; Jia, C.; Hou, Z.; Zhao, X.; Zhang, J.; Chang, W. Structural Insights into Energy Regulation of Light-Harvesting Complex CP29 from Spinach. *Nat. Struct. Mol. Biol.* **2011**, *18*, 309−315.

(26) Liu, Z.; Yan, H.; Wang, K.; Kuang, T.; Zhang, J.; Gui, L.; An, X.; Chang, W. Crystal Structure of Spinach Major Light-Harvesting Complex at 2.72 A Resolution. *Nature* **2004**, *428*, 287−292.

(27) Jansson, S. A Guide to the Lhc Genes and Their Relatives in Arabidopsis. *Trends Plant Sci.* **1999**, *4*, 236−240.